

1 **Genetic architecture underlying response to the fungal pathogen *Dothistroma septosporum***  
2 **in lodgepole pine, jack pine, and their hybrids**

3  
4 Mengmeng Lu<sup>1,2</sup>, Nicolas Feau<sup>3,4</sup>, Brandon Lind<sup>3</sup>, Dragana Obreht Vidakovic<sup>3</sup>, Pooja Singh<sup>1,5,6</sup>  
5 Sally N. Aitken<sup>3</sup>, Richard C. Hamelin<sup>3,7</sup>, and Sam Yeaman<sup>1</sup>

6 <sup>1</sup> Department of Biological Sciences, University of Calgary, 507 Campus Drive NW, Calgary,  
7 AB T2N 1N4, Canada

8  
9 <sup>2</sup> Department of Biological Sciences, University of Notre Dame, 100 Galvin Life Sciences, Notre  
10 Dame, IN 46556, USA

11  
12 <sup>3</sup> Department of Forest and Conservation Sciences, University of British Columbia, 3041-2424  
13 Main Mall, Vancouver, BC V6T 1Z4, Canada

14  
15 <sup>4</sup> Canadian Forest Service, Pacific Forestry Centre, Natural Resources Canada, Victoria, BC V8Z  
16 1M5, Canada

17  
18 <sup>5</sup> Aquatic Ecology & Evolution Division, Institute of Ecology and Evolution, University of Bern,  
19 Bern CH-3012, Switzerland

20  
21 <sup>6</sup> Center for Ecology, Evolution & Biogeochemistry, Swiss Federal Institute of Aquatic Science  
22 and Technology (EAWAG), Kastanienbaum CH-6047, Switzerland

23  
24 <sup>7</sup> Institut de Biologie Intégrative et des Systèmes, Université Laval, Pavillon Charles-Eugène-  
25 Marchand 1030, avenue de la Médecine, Québec City, Québec G1V 0A6, Canada

26  
27 **Correspondance**

28 Mengmeng Lu, Department of Biological Sciences, University of Calgary, 507 Campus Drive  
29 NW, Calgary, AB T2N 1N4, Canada

30  
31 Email : mengmeng.lu3510@gmail.com

32  
33 **ORCID**

34  
35 Mengmeng Lu <https://orcid.org/0000-0001-5023-3759>

36 Nicolas Feau <https://orcid.org/0000-0001-5925-9867>

37 Brandon Lind <https://orcid.org/0000-0002-8560-5417>

38 Pooja Singh <https://orcid.org/0000-0001-6576-400X>

39 Sally N. Aitken <https://orcid.org/0000-0002-2228-3625>

40 Richard C. Hamelin <https://orcid.org/0000-0003-4006-532X>

41 Sam Yeaman <https://orcid.org/0000-0002-1706-8699>

42

## 43 FUNDING INFORMATION

44 This research was supported by the CoAdapTree Project (241REF), with funding from Genome  
45 Canada, Genome BC, Genome Alberta, Genome Québec, the BC Ministry of Forests, Lands,  
46 Natural Resource Operations and Rural Development, and many other sponsors  
47 <http://adaptree.forestry.ubc.ca/sponsors/>, <http://coadaptree.forestry.ubc.ca/sponsors/>, and seed  
48 contributors <http://adaptree.forestry.ubc.ca/seed-contributors/>. Dr. Sam Yeaman is also funded  
49 by the Natural Sciences and Engineering Research Council of Canada (NSERC) and Alberta  
50 Innovates.

51

## 52 Abstract

53

54 In recent decades, *Dothistroma* needle blight (DNB), a pine tree disease caused by the fungal  
55 pathogen *Dothistroma septosporum*, has severely damaged lodgepole pine (*Pinus contorta*  
56 Dougl. ex. Loud.) in British Columbia, Canada, and raised health concerns for jack pine (*Pinus*  
57 *banksiana* Lamb.). The pathogen has already shown signs of host shift eastward to the hybrid  
58 populations between lodgepole pine and jack pine (*Pinus contorta*  $\times$  *P. banksiana*), and possibly  
59 into pure jack pine. However, we have little knowledge about mechanisms of resistance to *D.*  
60 *septosporum*, especially the underlying genetic basis of variation in pines. In this study, we  
61 conducted controlled inoculations to induce infection by *D. septosporum* and performed a  
62 genome-wide case-control association study with pooled sequencing (pool-seq) data to dissect  
63 the genetic architecture underlying response in lodgepole pine, jack pine, and their hybrids. We  
64 identified candidate genes associated with *D. septosporum* response in lodgepole pine and in  
65 hybrid samples. We also assessed genetic structure in hybrid populations and inferred how  
66 introgression may affect the distribution of genetic variation involved in *D. septosporum*  
67 response in the studied samples. These results can be used to develop genomic tools to evaluate  
68 DNB risk, guide forest management strategies, and potentially select for resistant genotypes.

69

70

## 71 KEY WORDS

72

73 Conifer, fungal pathogen resistance,  $F_{ST}$ , hybrid, introgression, pool-GWAS

74

75

## 76 1 | INTRODUCTION

77

78 Pests and pathogens constantly threaten forest trees, and their impacts are changing as climates  
79 are altered (Seidl et al., 2017; Simler-Williamson et al., 2019). Knowledge about the genetic  
80 architecture of pathogen resistance and the identified candidate resistance (R) genes provides the

81 basis for genomic breeding to improve tree resilience to forest pathogens. Genes and alleles that  
82 confer disease resistance or tolerance can eventually be used to develop genomic tools for  
83 rapidly selecting resistant genotypes (Isabel et al., 2019). Current breeding practices for forest  
84 trees involve recurrent selection, which includes repeated cycles of selection, breeding, and  
85 testing, to search for genotypes with better disease resistance, and then deployment of these  
86 selected tree genotypes (White, 2004). This takes years of effort to design and implement.  
87 Increasingly, genome editing is used to develop crops resistant to disease (van Esse et al., 2020).  
88 For fruit trees, CRISPR/Cas9 system has been applied to enhance the disease resistance in citrus  
89 (Jia et al., 2017; Wang et al., 2019), apple (Zhou et al., 2020), and others (Min et al., 2022).  
90 Given the long generation time in conifers and the frequent threats from diseases and insects,  
91 identifying R genes that can be targeted for selection or editing is a useful step in developing  
92 resistant genotypes for reforestation.  
93

94 *Dothistroma* needle blight (DNB), which is caused by the fungal pathogen *Dothistroma*  
95 *septosporum*, is a foliar disease of a wide range of pine trees (Gibson, 1972), with infected trees  
96 showing reddish-brown bands in needles, defoliation, and growth reduction. DNB has caused  
97 increased damage to lodgepole pine (*Pinus contorta* Dougl. ex. Loud., LP) in recent decades in  
98 Western Canada (Dale et al., 2011; Woods, 2003), and is now expanding its range eastwards,  
99 threatening jack pine (*Pinus banksiana* Lamb., JP). In severe cases, DNB causes extensive  
100 mortality, even amongst mature trees in LP plantations (Woods, 2003). Historically, DNB had  
101 only minor impacts on native forest trees in North America, but emerged as a severe forest  
102 disease during 1950s to 1960s in *Pinus radiata* plantations in Africa, New Zealand, and South  
103 America (Gibson, 1972). Recently, DNB has caused increased outbreak incidence and host range  
104 expansion in North America and Europe, which is likely correlated with climate change (Boroní  
105 et al., 2021; Welsh et al., 2009; Woods et al., 2005). In North America, while *D. septosporum*  
106 tends to be more common in moist western forests closer to the Pacific Ocean, *Dothistroma*-like  
107 symptoms were observed in drier forests of LP and natural hybrids between LP and JP (*Pinus*  
108 *contorta* × *P. banksiana*, LP × JP) in northern Alberta in 2012 and 2013 with further tests  
109 confirming *D. septosporum* was the cause of the disease observed (Ramsfield et al., 2021). Feau  
110 et al. (2021) performed a controlled inoculation experiment and demonstrated that LP, JP, and  
111 LP × JP are susceptible to *D. septosporum*, with JP showing a higher disease severity than LP or  
112 LP × JP, though there is no report showing DNB infection in natural JP forests. Considering *D.*  
113 *septosporum*'s eastward shift reaching towards the natural range of JP and JP's high  
114 susceptibility to *D. septosporum*, it is important to understand how these species respond to DNB  
115 infection.  
116

117 The evolutionary history and biogeography of JP and LP have likely played an important role in  
118 shaping the genetic basis of resistance to DNB. JP is widely distributed across boreal forests in  
119 eastern North America, extending in Canada from Northwest Territories to Nova Scotia  
120 (Rudolph & Laidly, 1990), areas largely outside of the historical range of *Dothistroma*. LP and  
121 JP evolved in allopatry, with an estimated divergence time of ~8 million years before present  
122 (Hao et al., 2015), but hybridized in areas of contact, primarily in central and northwestern  
123 Alberta (Burns et al., 2019; Rudolph & Yeatman, 1982). Following secondary contact of these  
124 two species, additional patchy regions of introgression have been developed in central Alberta  
125 north through to the Northwest Territories and northeastern British Columbia to the Alberta-  
126 Saskatchewan border (Burns et al., 2019). Natural LP × JP hybrids display a wide range of

127 phenotypes that are intermediate or more typical of one parent, depending on the level of  
128 introgression (Wood et al., 2009; Yeatman & Teich, 1969).

129  
130 In light of the geographic distribution of LP and JP, the longer history of host-pathogen  
131 coevolution in LP might explain its stronger resistance to DNB infection, compared to JP. A  
132 former study has evidenced coevolution between *Cronartium harknessii* lineages with LP and JP,  
133 with genetic basis underlying both pathogen virulence and host resistance (McAllister et al.,  
134 2022). For DNB infection caused by *D. septosporum*, though we lack direct evidence to prove a  
135 coevolutionary history between *D. septosporum* and different pine hosts, we have already  
136 identified candidate resistance genes to *D. septosporum* by RNA-seq analysis on experimentally  
137 infected LP seedlings (Lu et al., 2021). These candidate genes include 43 genes that are present  
138 in the plant-pathogen interaction pathway, as well as nine R genes that contained sites under  
139 positive selection. It seems that both constitutive (baseline) and induced (defenses activated after  
140 being attacked) defenses have been developed in LP. However, little is known about genetic  
141 basis of resistance to *D. septosporum* in JP. When subjected to other biotic agents, LP and JP  
142 showed unique monoterpene profiles in response to mountain pine beetle (Hall et al., 2013) and  
143 significant differences in chitinase gene expression in response to the fungal pathogens  
144 *Grosmannia clavigera* and *Cronartium harknessii* (Peery et al., 2021). These previous studies  
145 revealed the species-specific pathogen responses in a focused set of gene families. Nevertheless,  
146 since many complex traits are determined by many genes of small effect, to identify the causal  
147 genes underlying disease response traits, a genome-wide gene survey might give us a high-  
148 resolution perspective (Alonso-Blanco & Méndez-Vigo, 2014; Tam et al., 2019).

149  
150 To dissect the genetic architecture of pathogen resistance and to identify candidate genes,  
151 researchers have employed genetic markers, mainly SNPs, and methods like quantitative trait  
152 locus (QTL) mapping and genome-wide association analysis (GWAS). Polygenic disease  
153 responses, comprising numerous loci of small effect, appear to be the rule (Stocks et al., 2019).  
154 Large numbers of SNPs were associated with pitch canker resistance in *Pinus taeda* L. (De La  
155 Torre et al., 2019; Lu et al., 2017; Quesada et al., 2010), with white pine blister rust resistance in  
156 *Pinus lambertiana* Dougl. (Weiss et al., 2020), and with *Heterobasidion* root rot resistance in  
157 *Picea abies* (L.) Karst. (Capador-Barreto et al., 2021). To identify the candidate R genes, most  
158 GWAS studies on forest trees employ individual-based methods, with both phenotypic and  
159 genotypic data collected on each sampled individual. Case-control methods have been developed  
160 to study disease where individuals are pooled into healthy vs. infected groups, but such  
161 approaches typically still use individual-based sequencing to call genotypes before pooling (Wu  
162 et al., 2010). When multiple replicates are available, it is possible to combine pool-seq and the  
163 case-control design: Endler et al. (2016) analyzed the genetic differences underlying abdominal  
164 pigmentation variation among *Drosophila* populations, while Stocks et al. (2019) identified  
165 SNPs associated with low versus high ash dieback damage in *Fraxinus excelsior* L. using this  
166 approach. Recently, Singh et al. (2024) used a case-control pool-seq approach similar to that  
167 deployed here to search for signatures of resistance to Swiss needle cast in *Pseudotsuga*  
168 *menziesii* (Mirb.) Franco. Pool-seq is a cost-effective alternative approach to sequencing of  
169 individuals, but the weakness and limitations are also evident, such as unequal representation of  
170 individuals and suboptimal allele frequency estimate when the pool size is small, as well as  
171 misaligned mapping and sequencing errors (Schlötterer et al., 2014). Nonetheless, in a study on  
172 conifer genotyping, Lind et al. (2022) found that allele frequencies estimated from pooled DNA

173 sequencing samples were highly correlated with frequencies estimated from individual  
174 sequencing.

175  
176 Another factor in understanding the genetics of resistance is whether there is interplay between  
177 any alleles conferring resistance and introgression between the species. Bechsgaard et al. (2017)  
178 showed that plant R genes can adaptively introgress between closely related species. The LP × JP  
179 hybrid zone has been very well studied by Cullingham et al. (2012), who found that this hybrid  
180 zone presents a mosaic zone with variable introgression and patchy distributions of hybrids  
181 (Burns et al., 2019). While it is clear that these species share a broad hybrid zone, it is unclear  
182 whether any alleles for disease resistance will be more or less introgressed than the average  
183 region in the genome.

184  
185 In this study, our aim is to identify the genetic basis of DNB resistance in LP, JP, and LP × JP  
186 samples and to explore spatial patterning in any identified loci. The specific objectives of our  
187 study were to: 1) develop a GWAS case-control approach using pool-seq samples to identify loci  
188 with consistent associations with *D. septosporum* response across replicates; and 2) compare the  
189 genetic architecture underlying DNB resistance within the studied pine trees and infer how  
190 introgression may affect the genetic basis of *D. septosporum* responses. This study provides an  
191 important step towards identifying candidate genes to develop genomic tools for screening trees  
192 resistant to DNB infection.

193  
194 **2 | METHODS**  
195

196 **2.1 | Plant materials**

197 Seeds were obtained from 40 natural seedlots across Western Canada (Figure 1, seedlot numbers  
198 and locations can be found in Table S1, seed contributors [http://adaptree.forestry.ubc.ca/seed-  
199 contributors/](http://adaptree.forestry.ubc.ca/seed-contributors/)), including 25 LP seedlots from British Columbia (BC\_LP) and three from Alberta  
200 (AB\_LP), seven LP × JP seedlots from Alberta (AB\_LPxJP), and five JP seedlots from Alberta  
201 (AB\_JP). The range maps were downloaded from  
202 <https://sites.ualberta.ca/~ahamann/data/rangemaps.html> (Hamann et al., 2005). When the seeds  
203 were collected in the wild, they were assigned to pure LP, pure JP, or LP × JP, based on their  
204 location and morphological traits such as cone and branch characteristics, microfibril angle, and  
205 cell area (Wheeler & Guries, 1987; Wood et al., 2009; Yeatman & Teich, 1969). The proportion  
206 of LP and JP ancestry of the collected seeds were genotyped using 11 microsatellite loci by  
207 Cullingham et al. (2012). Briefly, seeds were germinated to obtain seedlings, then DNA was  
208 isolated from the seedlings. DNA was used to amplify 11 microsatellite loci and allele sizes were  
209 determined for genotyping as described by Cullingham et al. (2011).

210  
211 For the present study, seeds from the 40 seedlots were used to grow seedlings in a greenhouse at  
212 University of British Columbia, Vancouver, BC, for their first year (a flow chart of experimental  
213 procedure is shown in Figure S1). Resistance was phenotyped by inoculating 100 individuals per  
214 seedlot with one of two *D. septosporum* isolates (D1 & D2, 50 individuals of each isolate). D1  
215 was isolated from needles of an infected LP × JP seedlot in Alberta, Canada, while D2 was  
216 isolated from an infected LP seedlot in the Kispiox Valley region close to Smithers in  
217 Northwestern British Columbia, Canada (Feau et al., 2021; Ramsfield et al., 2021). The seedlots  
218 were identified as LP or LP × JP as aforementioned (Cullingham et al., 2012). The controlled

219 inoculation experiment was performed as described in Kabir et al. (2013) and Feau et al. (2021).  
220 Briefly, the one-year-old seedlings were placed in a completely randomized experimental design  
221 in a growth chamber with the condition of 16 hours daylight at 20 °C, 8 hours a night at 12 °C,  
222 and minimum relative humidity of 80 %. *D. septosporum* conidia were harvested from colonies  
223 grown for 10~16 days on *Dothistroma* sporulation medium plates and then suspended in sterile  
224 distilled water. Each seedling was sprayed twice at 10-day intervals with a standard inoculum of  
225 approximately 3 mL of  $1.6 \times 10^6$  conidia mL<sup>-1</sup>, using a household trigger action atomizer. Once  
226 the needles were dry (~45 minutes), the seedlings were wrapped in transparent plastic bags and  
227 kept in the growth chamber. After 48h the plastic bags were removed and the seedlings were  
228 kept in the growth chamber for 15 weeks till phenotyping. A mister spraying tap water was  
229 activated hourly for 3 minutes during the trial to maintain needle wetness. Control seedlings, at  
230 least one for each seedlot, were inoculated with sterile water.  
231

232 Fifteen weeks after inoculation, seedlings were rated for proportion of necrotic needles with red  
233 bands and/or fruiting bodies according to a disease severity scale of 1 to 5 (1 = least, 5 = most  
234 disease severity). Following disease rating, the ten most- and ten least-infected individuals per  
235 seedlot (five individuals for each *D. septosporum* isolate) were identified and retained for DNA  
236 extraction. Genomic DNA of each of these individuals was extracted as described in Lind et al.  
237 (2022), using the Nucleospin 96 Plant II Core kit (Macherey–Nagel GmbH & Co. KG, Germany)  
238 on an Eppendorf epMotion 5075 liquid-handling platform. The DNA of five most-infected and  
239 five least-infected individuals by each of the two *D. septosporum* isolates was combined in  
240 equimolar amounts to compose four pooled libraries per population, two susceptible (D1-S, D2-S)  
241 and two resistant libraries (D1-R, D2-R). Hence, 160 pooled DNA libraries were generated.  
242

## 243 2.2 | Sequence capture and pool-seq genotyping

244 The capture probes were comprised of two sets of probes. The first set of probes was designed  
245 based on an existing LP sequence capture array (Suren et al., 2016) by removing the probes that  
246 did not yield successful genotyping in Yeaman et al. (2016). Probe sequences of the existing  
247 capture array were aligned to the reference genome using GMAP v2019-03-15 (Wu & Watanabe,  
248 2005). Probes that covered the genomic regions with called SNPs in the dataset from Yeaman et  
249 al. (2016) were retained, otherwise the probes were discarded. Since there is no available LP  
250 reference genome, a masked *Pinus taeda* reference genome Pita.2\_01.masked3k2.fa  
251 (<https://treegenesdb.org/FTP/Genomes/Pita/v2.01/genome/>) (Neale et al., 2014) was used instead.  
252 *Pinus taeda* is a closely related species to LP (Jin et al., 2021). The second set of probes was  
253 newly designed probes derived from the *D. septosporum*-induced genes, which were based on a  
254 LP reference transcriptome assembled using the RNA-seq data of *D. septosporum* infected LP  
255 samples (Lu et al., 2021). To avoid duplicates, only those *D. septosporum*-induced genes with  
256 low homology to the retained probe sequences were used to design the new probes. To do so, the  
257 retained probe sequences were aligned to this transcriptome using blastn v2.9.0 with an E-value  
258 of 1e-10. A total of 8,778 *D. septosporum*-induced genes did not have any aligned probe  
259 sequences. These non-duplicate *D. septosporum*-induced genes were subsequently aligned to the  
260 reference genome to predict the exon-intron boundaries using GMAP v2019-03-15. Exon  
261 sequences from these induced genes with a length of at least 100 bp were combined with the  
262 previously designed working probe sequences, and this combined set of sequences was  
263 submitted to Roche NimbleGen (Roche Sequencing Solutions, Inc., CA USA) for Custom  
264 SeqCap EZ probe design (design name: 180321\_lodgepole\_v2\_EZ). Combining the two sets of

265 probes, this updated LP sequence capture array has a capture space of 44 Mbp, containing  
266 roughly 35,467 assembled genes. Most LP genes responsive to environment stress and fungal  
267 pathogen attack were included in the current capture probe design. Though genes expressed in  
268 different development periods might be missed, genes that have evidence of substantial  
269 expression have been covered in this capture probe design.  
270

271 The capture libraries for each of the 160 pools were constructed following NimbleGen SeqCap  
272 EZ Library SR User's Guide and as described in Lind et al. (2022). Then the R (resistant) and S  
273 (susceptible) libraries (two libraries per capture, R1+S1 or R2+S2, indexed with different  
274 barcodes) per population and per isolate were combined for sequence capture and enrichment.  
275 Sequencing was performed using the Illumina NovaSeq 6000 S4 PE 150 platform in Centre  
276 d'expertise et de services Génome Québec. Our in-house pool-seq pipeline (Lind, 2021) was  
277 employed to align the reads to the reference genome and call SNPs. For raw SNPs, only bi-allelic  
278 loci in regions without annotated repetitive elements or potentially paralogous genes were  
279 retained. The annotated repetitive elements were acquired from the LP genome annotation  
280 (Wegrzyn et al., 2014). The potentially paralogous genes were identified as described in Lind et  
281 al. (2022) using haploid megagametophyte sequences, for the heterozygous SNP calls for haploid  
282 sequences are likely to represent misalignments of paralogs. Afterwards, the SNP loci with depth  
283 (DP) < 10, DP > 400, global minor allele frequency < 0.05, or > 25% missing data were also  
284 removed.  
285

### 286 **2.3 | Genetic structure analyses**

287 The genetic structure among the 160 pooled samples, which represented four pooled libraries  
288 (D1-R, D1-S, D2-R, D2-S) for each of the 40 seedlots, was detected by using principal  
289 component analysis (PCA), reconstructing a phylogenetic tree, and by assessing correlation of  
290 allele frequencies and population differentiation ( $F_{ST}$ ) between samples using unlinked SNPs. To  
291 reduce the impact of linkage disequilibrium on estimation, the SNP set was thinned using  
292 vcftools (Danecek et al., 2011), so that no two sites were within 100,000 bp. PCA and genetic  
293 distance were calculated using the major allele depth and the R package "adegenet" (Jombart,  
294 2008). An unrooted phylogenetic tree was constructed using the distance output and the  
295 Neighbour-Joining algorithm, which was implemented by the R package "ape" (Paradis &  
296 Schliep, 2019). A bootstrap analysis was performed using 5000 bootstrap replicates. Correlation  
297 coefficients of major allele frequencies between all pairs within the 160 samples were calculated  
298 and plotted using the R package "corrplot" (Wei & Simko, 2017).  $F_{ST}$  was estimated between all  
299 pairs within the 160 samples using the R package "poolfstat" (Hivert et al., 2018). The clustering  
300 patterns output from these genetic structure analyses can be used to judge the subtle population  
301 structure leading to false positive problems in GWAS.  
302

### 303 **2.4 | Dissection of genetic architecture underlying *D. septosporum* response**

304 The alleles and candidate genes associated with *D. septosporum* response were detected using  
305 the pool-GWAS method. A GWAS case-control approach was developed using pool-seq samples  
306 to identify allele frequency differences between susceptible and resistant pines inoculated with *D.*  
307 *septosporum*. This method was based on Cochran-Mantel-Haenszel (CMH) method and  
308 implemented in our in-house pipeline (Lind, 2021). While sequencing read depth was commonly  
309 used as an estimation of allele count in such applications of test (Futschik & Schlötterer, 2010;  
310 Schlötterer et al., 2014), reliable results would be only achieved when the haploid size of the

311 sample is much greater than the depth of coverage (so that most reads arise from uniquely  
312 sampled haplotypes). As the pool size used in the present study (diploid size of 2N=10) is often  
313 smaller than the sequencing depth of coverage, read counts were converted into allele  
314 frequencies and then multiplied by the ploidy to yield an approximate count for each pool that  
315 represents the real replication level. A simulation was conducted to compare the false positive  
316 rate from the CMH test using uncorrected or corrected allele counts across a range of number of  
317 demes, individuals, and depths. Results showed that the false positive rate of the CMH method is  
318 high, especially when the sequencing depth is much higher than the pool size (Figure S2a).  
319 Using corrected allele counts, the allele frequencies multiplied by the ploidy (N=10) tends to  
320 lower the false positive rate (Figure S2b). Thus, the corrected allele counts were used for CMH  
321 test.  
322

323 As the genetic structure analysis showed that LP × JP and JP samples tend to cluster, JP samples  
324 and LP × JP samples were combined (JP + LP × JP) for downstream analyses. Pool-GWAS was  
325 performed separately within LP and JP + LP × JP samples. Analysis of R and S samples was  
326 conducted by combining individuals inoculated with D1 or D2 isolates to maximize statistical  
327 power. To identify candidate genes, SNPs in the top 1% of  $-\log_{10}(p)$  values from a pool-GWAS  
328 test were classified as outliers. As linkage disequilibrium can amplify signatures of selection,  
329 candidate resistance genes were identified as those with a large number of outlier SNPs relative  
330 to the average genome-wide expectation, as represented by an index based on the binomial  
331 distribution as per Yeaman et al. (2016). The identified loci on the enriched genes were realigned  
332 to the 12 LP linkage groups (MacLachlan et al., 2021) and Manhattan plots were drawn. The LP  
333 transcriptome (Lu et al., 2021) was used to annotate the reference genome. The aligned  
334 transcripts to the reference genome were identified as those with a minimum alignment identity  
335 of 90 % and a minimum alignment coverage of 85 % using GMAP v2019-03-15.  
336

## 337 **2.5 | Linkage disequilibrium (LD) between loci**

338 A non-linear model (Hill & Weir, 1988) was used to estimate the decay of LD with physical  
339 distance. Pairwise correlation ( $r^2$ ) of allele frequencies between loci on the same scaffold were  
340 calculated. The  $r^2$  values and the physical distances between loci on all scaffolds (genome-wide)  
341 or on scaffolds containing the identified top candidate genes (significant) were used to fit the  
342 non-linear model as described by Marroni et al. (2011). The LD decay graph was plotted using R  
343 (R Core Team, 2018).  
344

## 345 **2.6 | Introgression**

346 To study patterns of introgression affecting different regions of the genome and among different  
347 samples, the mean pairwise  $F_{ST}$  was calculated for each locus using the R package “poolfstat”.  
348 Loci with high  $F_{ST}$  values have high genetic differentiation, which may represent species barriers  
349 or genomic regions under divergent selection, while loci with low  $F_{ST}$  values imply introgression.  
350 To estimate genetic similarity of the studied JP and LP seedlots, the five JP samples (p36 to p40)  
351 and six pure LP samples (the six westmost LP samples, p15, p16, p18, p20, p23, p25) were used  
352 to calculate  $F_{ST}$  values, which were then averaged. To evaluate whether regions associated with  
353 *D. septosporum* response have atypical patterns of introgression, the  $F_{ST}$  values of the top 1 % *D.*  
354 *septosporum* response outliers identified from LP (N = 3,358) and those from JP + LP × JP (N =  
355 3,041) were compared, with  $F_{ST}$  values of randomly drawn SNPs (N = 3,400).

356 Similarly,  $F_{ST}$  between the JP + LP × JP samples (p29 to p40) and six pure LP samples (p15, p16,  
357 p18, p20, p23, p25) were averaged to estimate genetic similarity of the studied JP + LP × JP and  
358 LP. Different genomic regions were represented by different SNP sets, including *D. septosporum*  
359 response outliers identified from LP (N = 3,358) and outliers identified from JP + LP × JP (N =  
360 3,041), as well as the unlinked SNP set (N = 31,716), which was used in 2.3 for detecting genetic  
361 structure and representing random genomic region. The genetic similarity ( $F_{ST}$ ) of JP + LP × JP  
362 and LP was regressed to the longitude of these JP + LP × JP samples. The regression slopes for  
363 the three SNPs sets were compared using analysis of covariance method implemented by the R  
364 package “lsmeans” (Lenth, 2016; R Core Team, 2018).

365

### 366 3 | RESULTS

367

#### 368 3.1 | Patterns of genetic structure

369 After filtering, a total of 364,691 SNP loci were retained for downstream analyses, and most loci  
370 had a minor allele frequency between 0.05 and 0.1 (Figure S3). A thinned set of 31,716 unlinked  
371 SNPs was used for studying genetic structure among the 160 pooled samples (Figure 2). The  
372 most prominent patterns of structure were associated with species (Figure 2a & b, Figure S4),  
373 with LP samples readily distinguishable from JP and LP × JP samples. LP × JP samples clustered  
374 more closely with JP than LP. Compared to those sampled from the eastern hybrid zone, western  
375 LP × JP tend to be more similar to LP (samples were arranged according to longitude from left to  
376 right in Figure 2 c & d). Given this clear pattern of genetic structure, we conducted GWAS in LP  
377 and JP + LP × JP samples separately.

378

#### 379 3.2 | Signatures of association to infection response

380 Out of the 100 top-ranked candidate genes in each test (Table S2), three were identified within  
381 both the LP and JP + LP × JP samples (Figure 3). This is significantly more than the  
382 hypergeometric expectation, based on the probability of overlap for two draws of 100 genes from  
383 20,026 genes. A previous study anchored 10,093 scaffolds on the LP linkage map (MacLachlan  
384 et al., 2021), so we plotted SNPs and labeled the enriched plant-pathogen interaction candidate  
385 genes on the 12 linkage groups (Figure 3). The three genes identified in both species encode  
386 ABC transporter, F-box Kelch-repeat protein, and serine/threonine protein kinase. Genes  
387 encoding F-box protein and serine protein kinase were highlighted in Figure 3. Genes encoding  
388 ABC transporter were not included in the linkage groups, so they were not included in Figure 3.  
389 We also checked the enrichment of differentially expressed genes (DEGs) in the top 100 ranked  
390 genes. Out of 631 DEGs identified in the previous study (Lu et al., 2021), four were also  
391 candidate genes in the present study. Fisher’s Exact test showed there is no significant  
392 enrichment of DEGs in the candidate genes.

393

394 Loci on scaffolds with outliers (the SNPs with top 1 % of  $-\log_{10}(p)$  values from pool-GWAS test)  
395 tend to exhibit a more gradual decay in LD compared with the genome-wide loci on all scaffolds  
396 (Figure 4), with JP + LP × JP pine outliers having a much slower decay rate than LP. In LP, the  
397 distance at which LD decays to half of its maximum value is 96 bp for genome-wide loci, and  
398 174 bp for outlier loci. In JP + LP × JP, the half LD decay distance is 1,357 bp for genome-wide  
399 loci, and 68,215 bp for outlier loci. The slower LD decay pattern for the outliers may indicate  
400 selection on these identified loci.

401

402 **3.3 | Introgression**

403 By calculating average  $F_{ST}$  between pairs of LP and JP samples, we found that the *D.*  
404 *septosporum* response outliers, which were identified separately in LP or JP + LP  $\times$  JP samples,  
405 have higher  $F_{ST}$  values than randomly drawn SNPs (Wilcoxon test  $p$ -value < 0.01, Figure 5a &  
406 5b), with outliers identified in JP + LP  $\times$  JP samples showing higher  $F_{ST}$  values than those  
407 identified in LP samples (Wilcoxon test  $p$ -value < 0.01). These results suggest that the outliers  
408 associated with disease response constitute or are linked to genomic regions for divergent  
409 selection or species barriers, rather than facilitating introgression.  $F_{ST}$  estimates between JP + LP  
410  $\times$  JP samples and a set of pure LP samples showed a pattern of increased differentiation with  
411 distance eastwards of the JP + LP  $\times$  JP samples (Figure 5c), which were higher for the outliers  
412 than randomly chosen SNPs. Given the small number of samples, significance of linear model  
413 fitting is borderline, with  $p$ -value = 0.06 for outliers identified in LP,  $p$ -value = 0.05 for outliers  
414 identified in JP + LP  $\times$  JP, and  $p$ -value = 0.06 for randomly chosen SNPs (df = 10). The  
415 differences between regression slopes on different gene sets (LP outliers, JP + LP  $\times$  JP outliers,  
416 and unlinked SNPs) were not significant ( $p$ -values of pairwise comparisons > 0.3). Though it is  
417 not possible to test whether a linear vs. discontinuous model would fit better to these data, the  
418 results suggest that isolation-by-distance is occurring here.

419

420 **4 | DISCUSSION**

421

422 In recent decades, the fungal pathogen *D. septosporum* has become an increasing threat to LP in  
423 British Columbia (Feau et al., 2021; Welsh et al., 2009). Although *Dothistroma* needle blight  
424 (DNB) has not been observed in natural stands of JP in Alberta, Ramsfield et al. (2021)  
425 confirmed JP's susceptibility to infection by *D. septosporum* using a trial under natural  
426 conditions. The potential of climate change to allow this pathogen to spread across the wide  
427 natural distribution of JP raises serious concerns. The hybrid zone of contact between the sister  
428 species LP and JP may act as a bridge, allowing this fungal pathogen host shift (Taylor et al.,  
429 2015), as evidenced by the intermediate phenotype of gall development in LP  $\times$  JP seedlings  
430 compared to that in LP and JP (McAllister et al., 2022). The genetic basis of pathogen resistance  
431 in each species is therefore an important factor affecting the potential for host shift. To study the  
432 genetics of resistance to DNB, we analyzed the genetic architecture underlying *D. septosporum*  
433 response using the studied samples of LP, JP, and LP  $\times$  JP. We identified candidate genes  
434 associated with *D. septosporum* response and inferred the impact of introgression on the genetic  
435 structure underlying *D. septosporum* response in the studied samples. We detected largely non-  
436 overlapping sets of candidate genes in LP and JP + LP  $\times$  JP in response to *D. septosporum*,  
437 which might be shaped by different evolutionary forces of selection and introgression.  
438 Alternatively, the non-overlapping sets of candidate genes might reflect that many non-causal  
439 genes exist in the top 1 % GWAS outliers of each species, given that we did not test for  
440 significance at the gene-level. In either case, it seems clear that resistance to DNB is a highly  
441 polygenic trait with alleles of small effect.

442

443 This study is the first report of genome-wide scanning of *D. septosporum* response genes in LP,  
444 JP, and LP  $\times$  JP. We identified a few top candidate genes encoding leucine-rich repeats (LRR)-  
445 containing protein domain and serine threonine kinases in LP samples (Figure 3, Table S2). Plant  
446 breeders have long used nucleotide-binding LRR (NB-LRR) receptor R genes for preventing or

447 reducing diseases in crops. When attacked by infectious pathogens, plant NB-LRR receptors can  
448 recognize pathogen effectors by either direct or indirect mechanisms (Dodds & Rathjen, 2010).  
449 Such strategy is called effector-triggered immunity (ETI), which occurs after a basal resistance,  
450 pathogen-associated-molecular-patterns-triggered immunity (PTI). In a previous study using  
451 RNA-seq data, Lu et al. (2021) identified genes involved in PTI and ETI, as well as R genes with  
452 positive selection signals in LP. These results indicate that the long coevolutionary history  
453 between LP and *D. septosporum* (Capron et al., 2021; Welsh et al., 2009) has given rise to some  
454 tolerance or resistance mechanism against DNB. Since most of the identified associated markers  
455 are likely not causal but rather are in LD with the causal loci, the observed fast LD decay rate in  
456 lodgepole pine implies promising fine mapping resolutions as the identified markers are likely to  
457 be proximal to the causative genes.  
458

459 On the contrary, JP, as a potential new host, may not have coevolved such a specific defense, and  
460 the long LD blocks surrounding candidate genes identified from JP + LP × JP samples, which are  
461 typical of hybrid zones, limit the resolution of association mapping, so it may be difficult to  
462 locate the causative genes for follow-up studies (Goulet et al., 2017; Wilson & Goldstein, 2000).  
463 Additionally, we caution that the capture probes were designed using LP not JP genes,  
464 ascertainment bias might give rise to the underrepresentation of JP alleles (Lachance & Tishkoff,  
465 2013). However, we can use these JP + LP × JP candidate genes to infer how introgression  
466 affects the frequencies of disease-resistant alleles. Since we analyzed pool-seq data and lacked  
467 the pure JP samples out of the hybrid zone, it is not possible to analyze parental origin  
468 information, thus we inferred the ancestry using clustering. The clustering patterns in Figure 2  
469 show that most hybrid pine trees in our study had greater JP than LP ancestry, likely in part due  
470 to our limited sampling of JP from further Eastwards. Western LP × JP tend to be more  
471 genetically similar to LP, while eastern LP × JP tend to be more genetically dissimilar to LP.  
472 This is a typical characteristic for ongoing introgression and hybridization in the contact zone  
473 with a possible trend of LP expanding its range eastward (Harrison & Larson, 2014; Moran et al.,  
474 2021).  
475

476 In hybrid zones, alleles in some genomic regions are able to introgress across species boundaries,  
477 whereas alleles that constitute species barriers or are under divergent selection will remain  
478 differentiated (Harrison & Larson, 2014). We found significantly high  $F_{ST}$  values between JP and  
479 LP samples for the candidate genes associated with *D. septosporum* infection response. This can  
480 occur if these candidate genes tend to reside in genomic regions with restricted gene flow, driven  
481 by linkage with genes for divergent selection or species barriers. McAllister et al. (2022)  
482 observed a gradient of resistance to *C. harknessii* in LP, which could be associated with  
483 introgression of resistance genes from JP into LP. Since LP might have a long coevolutionary  
484 history with *D. septosporum* (Capron et al., 2021; Welsh et al., 2009), the introgression of LP  
485 genes into hybrids may increase resistance to *D. septosporum*. However, variation in  $F_{ST}$  along  
486 longitude (Figure 5c) did not differ significantly between background and candidate loci, so we  
487 cannot draw strong conclusions about adaptive introgression here.  
488

## 489 5 | CONCLUSION

490 The recent outbreaks of DNB in LP and its ability to infect JP pose a pressing need to  
491 understanding the genetic architecture of resistance to *D. septosporum*. The present study  
492 provides an array of candidate genes associated with *D. septosporum* response using pool-

493 GWAS. The identified candidate genes within LP and JP + LP × JP samples are largely non-  
494 overlapping, and the adaptive introgression is yet to be found. This knowledge can be used to  
495 develop genomic tools to minimize DNB risk and guide forest management strategies. Further  
496 testing and validation of these associations using a SNP array is currently underway.  
497  
498

## 499 FIGURE LEGENDS

500 FIGURE 1 Sampling locations (Table S1) of the 40 pine seedlots analyzed in this study, plotted  
501 within the natural range of *Pinus contorta* (lodgepole pine) and *Pinus banksiana* (jack pine) in  
502 Canada and USA. The top right map shows the context of the sampling locations. The range  
503 maps were downloaded from <https://sites.ualberta.ca/~ahamann/data/rangemaps.html>. BC\_LP  
504 (green diamonds) — *Pinus contorta* seedlots from British Columbia (N=25); AB\_LP (orange  
505 diamonds) — *Pinus contorta* seedlots from Alberta (N=3); AB\_LPxJP (purple diamonds) —  
506 *Pinus contorta* × *P. banksiana* hybrids seedlots from Alberta (N=7); AB\_JP (brown diamonds)  
507 — *Pinus banksiana* seedlots from Alberta (N=5).  
508

509 FIGURE 2 Genetic structure among the 160 pooled samples. a) Principal component analysis. b)  
510 Unrooted phylogenetic tree. The bootstrap values for each branch were shown in Figure S4. c)  
511 Correlation plot of the major allele frequencies between samples. d) Pairwise  $F_{ST}$  values between  
512 pools. BC\_LP — *Pinus contorta* (lodgepole pine) samples from British Columbia; AB\_LP —  
513 *Pinus contorta* (lodgepole pine) samples from Alberta; AB\_LPxJP — *Pinus contorta* × *P.*  
514 *banksiana* hybrids samples from Alberta; AB\_JP — *Pinus banksiana* (jack pine) samples from  
515 Alberta. D1 — *D. septosporum* isolate 1; D2 — *D. septosporum* isolate 2. R — resistant tree; S  
516 — susceptible tree. In c) and d), each column represents a pooled sample. The samples were  
517 arranged from left to right according to the longitude of sampling location, and four pooled  
518 libraries per seedlot (D1-R, D1-S, D2-R, D2-S) were arranged together.  
519

520 FIGURE 3 Manhattan plot showing SNPs associated with *D. septosporum* response within *Pinus*  
521 *contorta* (lodgepole pine, LP) and combined *Pinus banksiana* and *Pinus contorta* × *P. banksiana*  
522 hybrids (JP + LPxJP) samples. The x axis represents 12 linkage groups. The y axis represents  
523 significance of associations identified from pool-GWAS. Candidate genes were identified using  
524 a binomial test for enrichment of outlier SNPs per gene. Candidate genes and their surrounding  
525 50 kbp regions are highlighted in red. Of the three top-ranked candidate genes identified within  
526 both the LP and JP + LPxJP samples, one was not present in the linkage map, while the other  
527 two are highlighted in blue (“Serine” on linkage group 4 and “F-box” on linkage group 10).  
528 Labels in the graphs represent candidate genes encoding plant-pathogen interaction proteins:  
529 bHLH — bHLH transcription factor; Serine — serine/threonine-protein kinase; Auxin — auxin  
530 response factor; LRR — proteins with leucine-rich repeat; F-box — F-box Kelch-repeat protein;  
531 MADS — MADS transcription factor; MYB — MYB transcription factor; WRKY — WRKY  
532 transcription factor; TIF — translation initiation factor. The candidate gene IDs (in Table S2) are:  
533 In LP, bHLH — Scaffold\_2015-465162-569336; Serine\_1 — Scaffold\_3728-494595-736720;  
534 Serine\_2 — Scaffold\_3141-1-105566; Serine\_3 — Scaffold\_1072-1299306-1374553; Auxin —  
535 Scaffold\_3823-1571412-1689102; LRR — Scaffold\_1361-487806-570406; F-box —  
536 Scaffold\_3698-733755-839782; In JP + LPxJP, Serine — Scaffold\_3728-494595-736720;  
537 MADS — Scaffold\_427-2324701-2717580; F-box\_1 — Scaffold\_3698-733755-839782; MYB

538 — Scaffold\_4478-441537-627389; F-box\_2 — Scaffold\_342-1965787-2253515; WRKY —  
539 Scaffold\_830-1136302-1239031; TIF — Scaffold\_207-7583953-7695067.

540  
541 FIGURE 4 Linkage disequilibrium (LD) decay for genome-wide loci and outlier loci identified  
542 from *Pinus contorta* (lodgepole pine, LP) and combined *Pinus banksiana* and *Pinus contorta* × *P.*  
543 *banksiana* hybrids (JP + LPxJP) samples. The  $r^2$  values (pairwise correlation of allele  
544 frequencies between loci) and the physical distances between loci were used to fit the non-linear  
545 model as described by Marroni et al. (2011).

546  
547 FIGURE 5  $F_{ST}$  values of *D. septosporum* response outliers (a & b) and regression patterns of  $F_{ST}$   
548 values with longitude. For a & b, the  $F_{ST}$  values were calculated between the *Pinus banksiana*  
549 (jack pine, JP) samples (p36 to p40) and the six pure *Pinus contorta* (lodgepole pine, LP)  
550 samples (p15, p16, p18, p20, p23, p25).JP + LPxJP represents the combined JP and *Pinus*  
551 *contorta* × *P. banksiana* hybrids samples.  $F_{ST}$  values of *D. septosporum* response outliers  
552 identified from LP (N=3,358) and JP + LPxJP (N=3,041) samples were compared, with  $F_{ST}$   
553 values of randomly drawn SNPs (N=3,400). Outliers identified from both species have higher  
554  $F_{ST}$  values than randomly drawn SNPs ( $p$ -value < 0.01). For c, the  $F_{ST}$  values were calculated  
555 between the JP + LPxJP samples (p29 to p40) and the six pure LP samples (p15, p16, p18, p20,  
556 p23, p25) and then averaged for each JP + LPxJP sample. Different genomic regions were  
557 represented by different SNP sets, including LP outliers (N=3,358), JP + LPxJP outliers  
558 (N=3,041), and unlinked SNPs (N=31,716). The  $F_{ST}$  values represented by different SNP sets  
559 were regressed to the longitude of these JP + LPxJP samples. Differences between slopes are not  
560 significant (ANCOVA,  $p$ -value > 0.3).

561  
562 **AUTHOR CONTRIBUTIONS**

563 Mengmeng Lu and Sam Yeaman conceived analyses and wrote the manuscript. Mengmeng Lu  
564 performed computational analyses. Nicolas Feau and Richard C. Hamelin designed pathogen  
565 inoculation and phenotyping protocol. Nicolas Feau performed the pathogen inoculation and  
566 phenotyping in the greenhouse. Brandon Lind and Pooja Singh designed pool-GWAS analyses  
567 pipeline. Dragana Obreht Vidakov performed sequence capture work. Sally N. Aitken, Richard C.  
568 Hamelin, and Sam Yeaman obtained funding. All authors edited the manuscript.

569  
570  
571 **ACKNOWLEDGMENTS**

572 We thank Centre d'expertise et de services Génome Québec for sequencing service, University of  
573 Calgary Information Technologies for system support, the Research Oversight Committee of  
574 CoAdapTree Project for suggestions and help. Special gratitude goes to Dr. Andy Benowicz and  
575 our seed contributors <http://adaptree.forestry.ubc.ca/seed-contributors/>.

576  
577 **CONFLICT OF INTEREST STATEMENT**

578 The authors declare no conflict of interest.

579  
580

581 **DATA AVAILABILITY STATEMENT**

582 The raw pool-seq data were deposited in NCBI SRA (accession number: PRJNA602898;  
583 <http://www.ncbi.nlm.nih.gov/sra>). The assembled transcriptomes and their annotation were  
584 deposited in Dryad <https://doi.org/10.5061/dryad.prr4xgxtk>. The scripts used for analyses  
585 were deposited in <https://github.com/Mengmeng-Lu/Genetic-architecture-underlying-response-to-the-fungal-pathogen-Dothistroma-septosporum-in-Pinus-con>

587

588

## 589 REFERENCES

590

591 Alonso-Blanco, C. & Méndez-Vigo, B. (2014). Genetic architecture of naturally occurring  
592 quantitative traits in plants: an updated synthesis. *Current opinion in plant biology*, 18,  
593 37-43. <https://doi.org/10.1016/j.pbi.2014.01.002>

594 Bechsgaard, J., Jorgensen, T. H., & Schierup, M. H. (2017). Evidence for adaptive introgression of  
595 disease resistance genes among closely related *Arabidopsis* species. *G3 (Bethesda)*, 7(8),  
596 2677-2683. <https://doi.org/10.1534/g3.117.043984>

597 Boroń, P., Lenart-Boroń, A., Mullett, M., Grad, B., & Nawrot-Chorabik, K. (2021). Population  
598 structure of *Dothistroma septosporum* in Poland: revealing the genetic signature of a  
599 recently established pathogen. *Plant Pathology*, 70(6), 1310-1325.  
600 <https://doi.org/10.1111/ppa.13383>

601 Burns, I., James, P. M. A., Coltman, D. W., & Cullingham, C. I. (2019). Spatial and genetic  
602 structure of the lodgepole x jack pine hybrid zone. *Canadian Journal of Forest Research*,  
603 49(7), 844-853. <https://doi.org/10.1139/cjfr-2018-0428>

604 Capador-Barreto, H. D., Bernhardsson, C., Milesi, P., Vos, I., Lundén, K., Wu, H. X., . . . Elfstrand,  
605 M. (2021). Killing two enemies with one stone? Genomics of resistance to two sympatric  
606 pathogens in Norway spruce. *Molecular Ecology*, 30(18), 4433-4447.  
607 <https://doi.org/10.1111/mec.16058>

608 Capron, A., Feau, N., Heinzelmann, R., Barnes, I., Benowicz, A., Bradshaw, R. E., . . . Hamelin, R.  
609 C. (2021). Signatures of post-glacial genetic isolation and human-driven migration in the  
610 *Dothistroma* needle blight pathogen in Western Canada. *Phytopathology*, 111(1), 116-  
611 127. <https://doi.org/10.1094/phyto-08-20-0350-fi>

612 Cullingham, C. I., Cooke, J. E., Dang, S., Davis, C. S., Cooke, B. J., & Coltman, D. W. (2011).  
613 Mountain pine beetle host-range expansion threatens the boreal forest. *Molecular  
614 Ecology*, 20(10), 2157-2171. <https://doi.org/10.1111/j.1365-294X.2011.05086.x>

615 Cullingham, C. I., James, P. M., Cooke, J. E., & Coltman, D. W. (2012). Characterizing the physical  
616 and genetic structure of the lodgepole pine x jack pine hybrid zone: mosaic structure and  
617 differential introgression. *Evolutionary Applications*, 5(8), 879-891.  
618 <https://doi.org/10.1111/j.1752-4571.2012.00266.x>

619 Dale, A. L., Lewis, K. J., & Murray, B. W. (2011). Sexual reproduction and gene flow in the pine  
620 pathogen *Dothistroma septosporum* in British Columbia. *Phytopathology*, 101(1), 68-76.  
621 <https://doi.org/10.1094/phyto-04-10-0121>

622 Danecek, P., Auton, A., Abecasis, G., Albers, C. A., Banks, E., DePristo, M. A., . . . 1000 Genomes  
623 Project Analysis Group. (2011). The variant call format and VCFtools. *Bioinformatics*,  
624 27(15), 2156-2158. <https://doi.org/10.1093/bioinformatics/btr330>

625 De La Torre, A. R., Puiu, D., Crepeau, M. W., Stevens, K., Salzberg, S. L., Langley, C. H., & Neale,  
626 D. B. (2019). Genomic architecture of complex traits in loblolly pine. *New Phytologist*,  
627 221(4), 1789-1801. <https://doi.org/10.1111/nph.15535>

628 Dodds, P. N. & Rathjen, J. P. (2010). Plant immunity: towards an integrated view of plant–  
629 pathogen interactions. *Nature review genetics*, 11(8), 539-548.  
630 <https://doi.org/10.1038/nrg2812>

631 Endler, L., Betancourt, A. J., Nolte, V., & Schlötterer, C. (2016). Reconciling differences in pool-  
632 GWAS between populations: A case study of female abdominal pigmentation in  
633 *Drosophila melanogaster*. *Genetics*, 202(2), 843-855.  
634 <https://doi.org/10.1534/genetics.115.183376>

635 Feau, N., Ramsfield, T. D., Myrholm, C. L., Tomm, B., Cerezke, H. F., Benowicz, A., . . . Hamelin, R.  
636 C. (2021). DNA-barcoding identification of *Dothistroma septosporum* on *Pinus contorta*  
637 var. *latifolia*, *P. banksiana* and their hybrid in northern Alberta, Canada. *Canadian*  
638 *Journal of Plant Pathology*, 43(3), 472-479.  
639 <https://doi.org/10.1080/07060661.2020.1829065>

640 Futschik, A. & Schlötterer, C. (2010). The next generation of molecular markers from massively  
641 parallel sequencing of pooled DNA Samples. *Genetics*, 186(1), 207-218.  
642 <https://doi.org/10.1534/genetics.110.114397>

643 Gibson, I. A. S. (1972). Dothistroma Blight of *Pinus Radiata*. *Annual Review of Phytopathology*,  
644 10(1), 51-72. <https://doi.org/10.1146/annurev.py.10.090172.000411>

645 Goulet, B. E., Roda, F., & Hopkins, R. (2017). Hybridization in plants: Old ideas, new techniques.  
646 *Plant physiology*, 173(1), 65-78. <https://doi.org/10.1104/pp.16.01340>

647 Hall, D. E., Yuen, M. M. S., Jancsik, S., Quesada, A. L., Dullat, H. K., Li, M., . . . Bohlmann, J. (2013).  
648 Transcriptome resources and functional characterization of monoterpene synthases for  
649 two host species of the mountain pine beetle, lodgepole pine (*Pinus contorta*) and jack  
650 pine (*Pinus banksiana*). *BMC plant biology*, 13(1), 80. <https://doi.org/10.1186/1471-2229-13-80>

651 Hamann, A., Smets, P., Yanchuk, A. D., & Aitken, S. N. (2005). An ecogeographic framework for  
652 in situ conservation of forest trees in British Columbia. *Canadian Journal of Forest  
653 Research*, 35(11), 2553-2561. <https://doi.org/10.1139/x05-181>

654 Hao, Z.-Z., Liu, Y.-Y., Nazaire, M., Wei, X.-X., & Wang, X.-Q. (2015). Molecular phylogenetics and  
655 evolutionary history of sect. *Quinquefoliae* (*Pinus*): Implications for Northern  
656 Hemisphere biogeography. *Molecular Phylogenetics and Evolution*, 87, 65-79.  
657 <https://doi.org/10.1016/j.ympev.2015.03.013>

658 Harrison, R. G. & Larson, E. L. (2014). Hybridization, introgression, and the nature of species  
659 boundaries. *Journal of Heredity*, 105(S1), 795-809.  
660 <https://doi.org/10.1093/jhered/esu033>

661 Hill, W. G. & Weir, B. S. (1988). Variances and covariances of squared linkage disequilibria in  
662 finite populations. *Theoretical population biology*, 33(1), 54-78.  
663 [https://doi.org/10.1016/0040-5809\(88\)90004-4](https://doi.org/10.1016/0040-5809(88)90004-4)

664 Hivert, V., Leblois, R., Petit, E. J., Gautier, M., & Vitalis, R. (2018). Measuring genetic  
665 differentiation from pool-seq data. *Genetics*, 210(1), 315-330.  
666 <https://doi.org/10.1534/genetics.118.300900>

667

668 Isabel, N., Holliday, J. A., & Aitken, S. N. (2019). Forest genomics: Advancing climate adaptation,  
669 forest health, productivity, and conservation. *Evolutionary Applications*, 13(1), 3-10.  
670 <https://doi.org/10.1111/eva.12902>

671 Jia, H., Zhang, Y., Orbović, V., Xu, J., White, F. F., Jones, J. B., & Wang, N. (2017). Genome editing  
672 of the disease susceptibility gene *CsLOB1* in citrus confers resistance to citrus canker.  
673 *Plant biotechnology journal*, 15(7), 817-823. <https://doi.org/10.1111/pbi.12677>

674 Jin, W.-T., Gernandt, D. S., Wehenkel, C., Xia, X.-M., Wei, X.-X., & Wang, X.-Q. (2021).  
675 Phylogenomic and ecological analyses reveal the spatiotemporal evolution of global  
676 pines. *Proceedings of the National Academy of Sciences*, 118(20), e2022302118.  
677 <https://doi.org/10.1073/pnas.2022302118>

678 Jombart, T. (2008). adegenet: a R package for the multivariate analysis of genetic markers.  
679 *Bioinformatics*, 24(11), 1403-1405. <https://doi.org/10.1093/bioinformatics/btn129>

680 Kabir, M. S., Ganley, R. J., & Bradshaw, R. E. (2013). An improved artificial pathogenicity assay  
681 for *Dothistroma* needle blight on *Pinus radiata*. *Australasian Plant Pathology*, 42(4),  
682 503-510. <https://doi.org/10.1007/s13313-013-0217-z>

683 Lachance, J. & Tishkoff, S. A. (2013). SNP ascertainment bias in population genetic analyses:  
684 why it is important, and how to correct it. *Bioessays*, 35(9), 780-786.  
685 <https://doi.org/10.1002/bies.201300014>

686 Lenth, R. V. (2016). Least-squares means: The R package lsmeans. *Journal of Statistical Software*,  
687 69(1), 1 - 33. <https://doi.org/10.18637/jss.v069.i01>

688 Lind, B. M. (2021). GitHub.com/brandonlind/cmh\_test: preprint release (Version 1.0.0). Zenodo.  
689 <http://doi.org/10.5281/zenodo.5083798>

690 Lind, B. M. (2021). GitHub.com/CoAdapTree/varscan\_pipeline: Publication release (Version  
691 1.0.0). Zenodo. <https://doi.org/10.5281/zenodo.5083302>

692 Lind, B. M., Lu, M., Obreht Vidakovic, D., Singh, P., Booker, T. R., Aitken, S. N., & Yeaman, S.  
693 (2022). Haploid, diploid, and pooled exome capture recapitulate features of biology and  
694 paralogy in two non-model tree species. *Molecular Ecology Resources*, 22(1), 225-238.  
695 <https://doi.org/10.1111/1755-0998.13474>

696 Lu, M., Feau, N., Obreht Vidakovic, D., Ukrainetz, N., Wong, B., Aitken, S. N., . . . Yeaman, S.  
697 (2021). Comparative gene expression analysis reveals mechanism of *Pinus contorta*  
698 response to the fungal pathogen *Dothistroma septosporum*. *Molecular plant-microbe  
699 interactions: MPMI*, 34(4), 397-409. <https://doi.org/10.1094/mpmi-10-20-0282-r>

700 Lu, M., Krutovsky, K. V., Nelson, C. D., West, J. B., Reilly, N. A., & Loopstra, C. A. (2017).  
701 Association genetics of growth and adaptive traits in loblolly pine (*Pinus taeda* L.) using  
702 whole-exome-discovered polymorphisms. *Tree Genetics & Genomes*, 13(3), 57.  
703 <https://doi.org/10.1007/s11295-017-1140-1>

704 MacLachlan, I. R., McDonald, T. K., Lind, B. M., Rieseberg, L. H., Yeaman, S., & Aitken, S. N.  
705 (2021). Genome-wide shifts in climate-related variation underpin responses to selective  
706 breeding in a widespread conifer. *Proceedings of the National Academy of Sciences*,  
707 118(10), e2016900118. <https://doi.org/10.1073/pnas.2016900118>

708 Marroni, F., Pinosio, S., Zaina, G., Fogolari, F., Felice, N., Cattonaro, F., & Morgante, M. (2011).  
709 Nucleotide diversity and linkage disequilibrium in *Populus nigra* cinnamyl alcohol  
710 dehydrogenase (CAD4) gene. *Tree Genetics & Genomes*, 7(5), 1011-1023.  
711 <https://doi.org/10.1007/s11295-011-0391-5>

712 McAllister, C. H., Cullingham, C. I., Peery, R. M., Mbenoun, M., McPeak, E., Feau, N., . . . Cooke, J.  
713 E. K. (2022). Evidence of coevolution between *Cronartium harknessii* lineages and their  
714 corresponding hosts, lodgepole pine and jack pine. *Phytopathology*, 112(8), 1795-1807.  
715 <https://doi.org/10.1094/phyto-09-21-0370-r>

716 Min, T., Hwarari, D., Li, D., Movahedi, A., & Yang, L. (2022). CRISPR-based genome editing and  
717 its applications in woody plants. *International journal of molecular sciences*, 23(17),  
718 10175. <https://doi.org/10.3390/ijms231710175>

719 Moran, B. M., Payne, C., Langdon, Q., Powell, D. L., Brandvain, Y., & Schumer, M. (2021). The  
720 genomic consequences of hybridization. *eLife*, 10, e69016.  
721 <https://doi.org/10.7554/eLife.69016>

722 Neale, D. B., Wegrzyn, J. L., Stevens, K. A., Zimin, A. V., Puiu, D., Crepeau, M. W., . . . Langley, C.  
723 H. (2014). Decoding the massive genome of loblolly pine using haploid DNA and novel  
724 assembly strategies. *Genome Biology*, 15(3), R59. <https://doi.org/10.1186/gb-2014-15-3-r59>

725 Paradis, E. & Schliep, K. (2019). ape 5.0: an environment for modern phylogenetics and  
726 evolutionary analyses in R. *Bioinformatics*, 35(3), 526-528.  
727 <https://doi.org/10.1093/bioinformatics/bty633>

728 Peery, R. M., McAllister, C. H., Cullingham, C. I., Mahon, E. L., Arango-Velez, A., & Cooke, J. E. K.  
729 (2021). Comparative genomics of the chitinase gene family in lodgepole and jack pines:  
730 contrasting responses to biotic threats and landscape level investigation of genetic  
731 differentiation. *Botany*, 99(6), 355-378. <https://doi.org/10.1139/cjb-2020-0125>

732 Quesada, T., Gopal, V., Cumbie, W. P., Eckert, A. J., Wegrzyn, J. L., Neale, D. B., . . . Davis, J. M.  
733 (2010). Association mapping of quantitative disease resistance in a natural population of  
734 loblolly pine (*Pinus taeda* L.). *Genetics*, 186(2), 677-686.  
735 <https://doi.org/10.1534/genetics.110.117549>

736 R Core Team. (2018). R: A language and environment for statistical computing. Vienna, Austria:  
737 R Foundation for Statistical Computing. <https://www.R-project.org/>

738 Ramsfield, T., Myrholm, C., & Tomm, B. (2021). Natural infection of *Pinus contorta* var. *latifolia*,  
739 *Pinus banksiana* and their hybrid by *Dothistroma septosporum* in Alberta, Canada.  
740 *Forest Pathology*, 51(5), e12717. <https://doi.org/10.1111/efp.12717>

741 Rudolph, T. D. & Laidly, P. R. (1990). *Pinus banksiana* Lamb. Jack Pine. In R. M. Burns & B. H.  
742 Honkala (Eds.), *Silvics of North America* (Vol. Volume 1: Conifers. Agriculture Handbook  
743 654, pp. 280-293). Washington, D.C.: USDA Forest Service.

744 Rudolph, T. D. & Yeatman, C. W. (1982). Genetics of jack pine. In *Research Paper WO-38* (pp.  
745 35-37). Washington, D.C.: USDA Forest Service.

746 Schlotterer, C., Tobler, R., Kofler, R., & Nolte, V. (2014). Sequencing pools of individuals —  
747 mining genome-wide polymorphism data without big funding. *Nature Reviews Genetics*,  
748 15(11), 749-763. <https://doi.org/10.1038/nrg3803>

749 Seidl, R., Thom, D., Kautz, M., Martin-Benito, D., Peltoniemi, M., Vacchiano, G., . . . Reyer, C. P.  
750 O. (2017). Forest disturbances under climate change. *Nature Climate Change*, 7(6), 395-  
751 402. <https://doi.org/10.1038/nclimate3303>

752 Simler-Williamson, A. B., Rizzo, D. M., & Cobb, R. C. (2019). Interacting effects of global change  
753 on forest pest and pathogen dynamics. *Annual Review of Ecology, Evolution, and  
754 Systematics*, 50, 381-403. <https://doi.org/10.1146/annurev-ecolsys-110218-024934>

756 Singh, P., St Clair, J. B., Lind, B. M., Cronn, R., Wilhelmi, N. P., Feau, N., . . . Yeaman, S. (2024).  
757       Genetic architecture of disease resistance and tolerance in Douglas-fir trees. *New*  
758       *Phytologist*, 243(2), 705-719. <https://doi.org/10.1111/nph.19797>

759 Stocks, J. J., Metheringham, C. L., Plumb, W. J., Lee, S. J., Kelly, L. J., Nichols, R. A., & Buggs, R. J.  
760       A. (2019). Genomic basis of European ash tree resistance to ash dieback fungus. *Nature*  
761       *Ecology & Evolution*, 3(12), 1686-1696. <https://doi.org/10.1038/s41559-019-1036-6>

762 Suren, H., Hodgins, K. A., Yeaman, S., Nurkowski, K. A., Smets, P., Rieseberg, L. H., . . . Holliday, J.  
763       A. (2016). Exome capture from the spruce and pine giga-genomes. *Molecular Ecology*  
764       *Resources*, 16(5), 1136-1146. <https://doi.org/10.1111/1755-0998.12570>

765 Tam, V., Patel, N., Turcotte, M., Bossé, Y., Paré, G., & Meyre, D. (2019). Benefits and limitations  
766       of genome-wide association studies. *Nature Reviews Genetics*, 20(8), 467-484.  
767       <https://doi.org/10.1038/s41576-019-0127-1>

768 Taylor, S. A., Larson, E. L., & Harrison, R. G. (2015). Hybrid zones: windows on climate change.  
769       *Trends in Ecology & Evolution*, 30(7), 398-406.  
770       <https://doi.org/10.1016/j.tree.2015.04.010>

771 van Esse, H. P., Reuber, T. L., & van der Does, D. (2020). Genetic modification to improve  
772       disease resistance in crops. *New Phytologist*, 225(1), 70-86.  
773       <https://doi.org/10.1111/nph.15967>

774 Wang, L., Chen, S., Peng, A., Xie, Z., He, Y., & Zou, X. (2019). CRISPR/Cas9-mediated editing of  
775       CsWRKY22 reduces susceptibility to *Xanthomonas citri* subsp. *citri* in Wanjincheng  
776       orange (*Citrus sinensis* (L.) Osbeck). *Plant Biotechnology Reports*, 13(5), 501-510.  
777       <https://doi.org/10.1007/s11816-019-00556-x>

778 Wegrzyn, J. L., Liechty, J. D., Stevens, K. A., Wu, L. S., Loopstra, C. A., Vasquez-Gross, H. A., . . .  
779       Neale, D. B. (2014). Unique features of the loblolly pine (*Pinus taeda* L.) megagenome  
780       revealed through sequence annotation. *Genetics*, 196(3), 891-909.  
781       <https://doi.org/10.1534/genetics.113.159996>

782 Wei, T. & Simko, V. (2017). R package “corrplot”: Visulaization of a correlation matrix.  
783       <https://github.com/taiyun/corrplot>

784 Weiss, M., Sniezko, R. A., Puiu, D., Crepeau, M. W., Stevens, K., Salzberg, S. L., . . . De La Torre, A.  
785       R. (2020). Genomic basis of white pine blister rust quantitative disease resistance and its  
786       relationship with qualitative resistance. *The Plant Journal*, 104(2), 365-376.  
787       <https://doi.org/10.1111/tpj.14928>

788 Welsh, C., Lewis, K., & Woods, A. (2009). The outbreak history of *Dothistroma* needle blight: an  
789       emerging forest disease in northwestern British Columbia, Canada. *Canadian Journal of*  
790       *Forest Research*, 39(12), 2505-2519. <https://doi.org/10.1139/X09-159>

791 Wheeler, N. C. & Guries, R. P. (1987). A quantitative measure of introgression between  
792       lodgepole and jack pines. *Canadian Journal of Botany*, 65, 1876-1885.  
793       <https://doi.org/10.1139/b87-257>

794 White, T. L. (2004). TREE BREEDING, PRINCIPLES | Breeding Theory and Genetic Testing. In J.  
795       Burley (Ed.), *Encyclopedia of Forest Sciences* (pp. 1551-1561). University of Oxford,  
796       Oxford, UK: Elsevier.

797 Wilson, J. F. & Goldstein, D. B. (2000). Consistent long-range linkage disequilibrium generated  
798       by admixture in a Bantu-Semitic hybrid population. *The American Journal of Human*  
799       *Genetics*, 67(4), 926-935. <https://doi.org/10.1086/303083>

800 Wood, L. J., Hartley, I. D., & Watson, P. (2009). Determining hybridization in jack pine and  
801 lodgepole pine from British Columbia. *Wood and Fiber Science*, 41, 386-395.

802 Woods, A. J. (2003). Species diversity and forest health in northwest British Columbia. *The*  
803 *Forestry Chronicle*, 79(5), 892-897. <https://doi.org/10.5558/tfc79892-5>

804 Woods, A. J., Coates, K. D., & Hamann, A. (2005). Is an unprecedented *Dothistroma* needle  
805 blight epidemic related to climate change? *BioScience*, 55(9), 761-769.  
806 [https://doi.org/10.1641/0006-3568\(2005\)055\[0761:IAUDNB\]2.0.CO;2](https://doi.org/10.1641/0006-3568(2005)055[0761:IAUDNB]2.0.CO;2)

807 Wu, M. C., Kraft, P., Epstein, M. P., Taylor, D. M., Chanock, S. J., Hunter, D. J., & Lin, X. (2010).  
808 Powerful SNP-set analysis for case-control genome-wide association studies. *American*  
809 *Journal of Human Genetics*, 86(6), 929-942. <https://doi.org/10.1016/j.ajhg.2010.05.002>

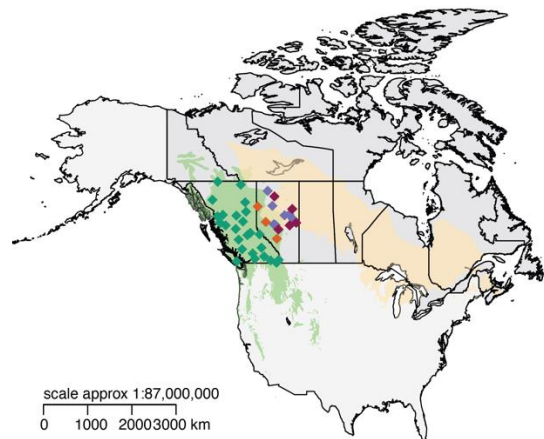
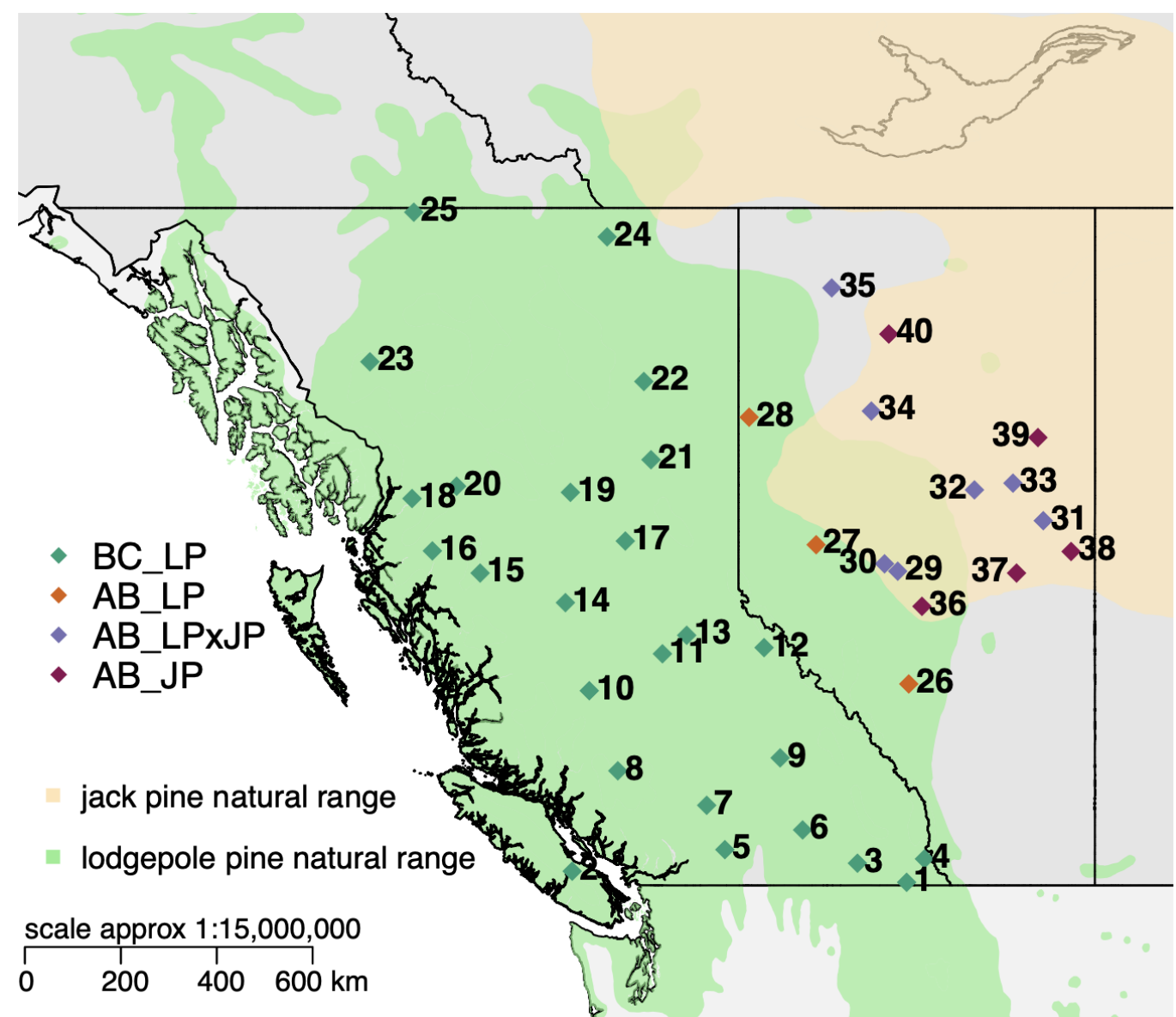
810 Wu, T. D. & Watanabe, C. K. (2005). GMAP: a genomic mapping and alignment program for  
811 mRNA and EST sequences. *Bioinformatics*, 21(9), 1859-1875.  
812 <https://doi.org/10.1093/bioinformatics/bti310>

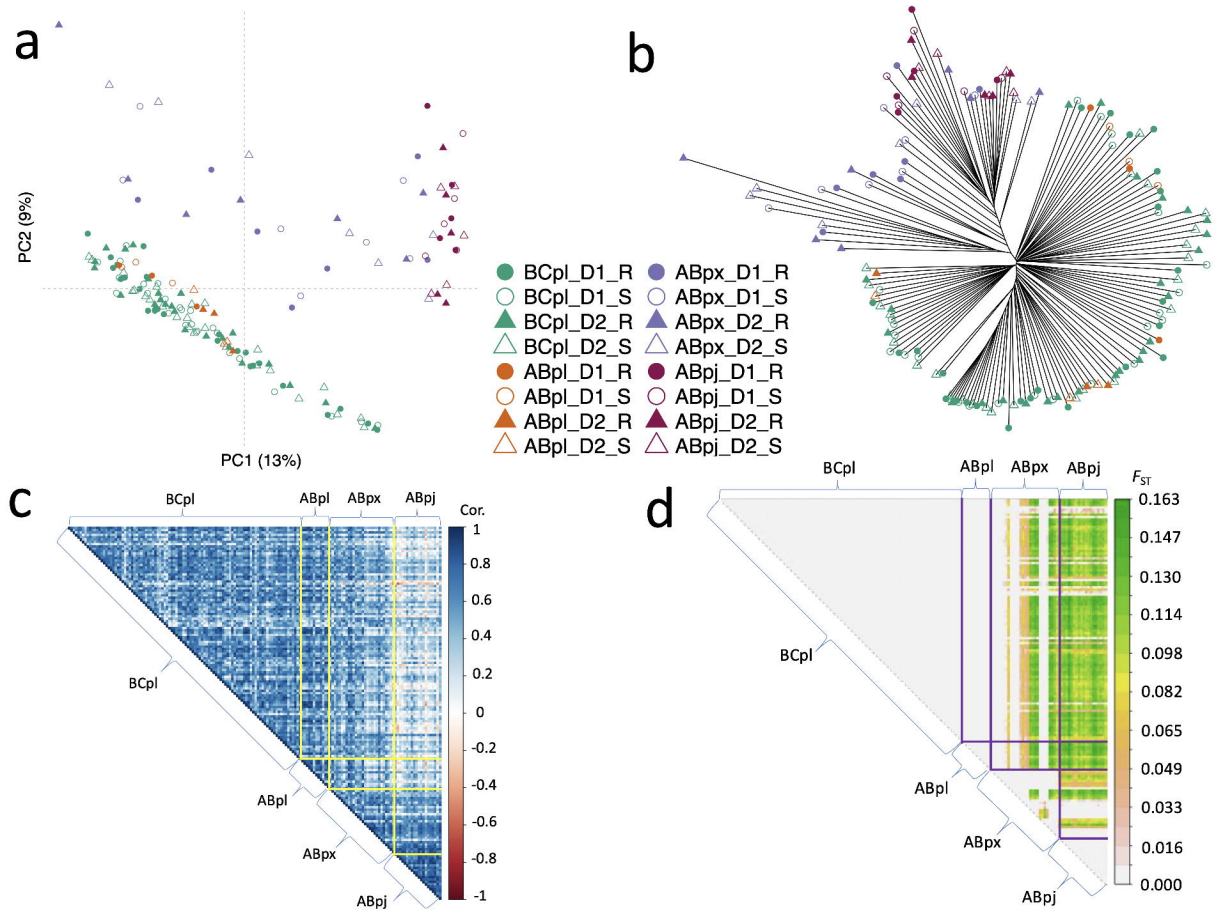
813 Yeaman, S., Hodgins, K. A., Lotterhos, K. E., Suren, H., Nadeau, S., Degner, J. C., . . . Aitken, S. N.  
814 (2016). Convergent local adaptation to climate in distantly related conifers. *Science*,  
815 353(6306), 1431-1433. <https://doi.org/10.1126/science.aaf7812>

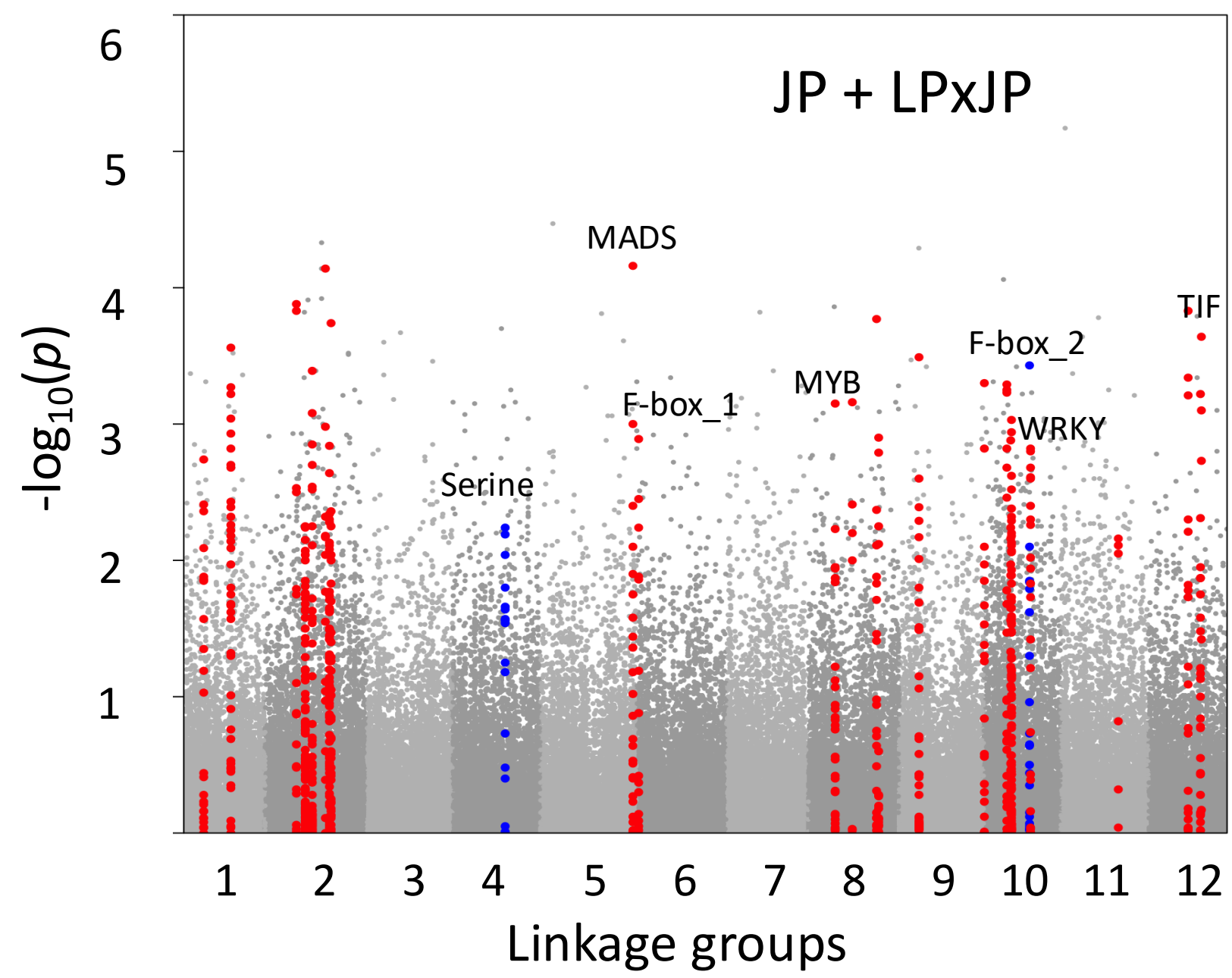
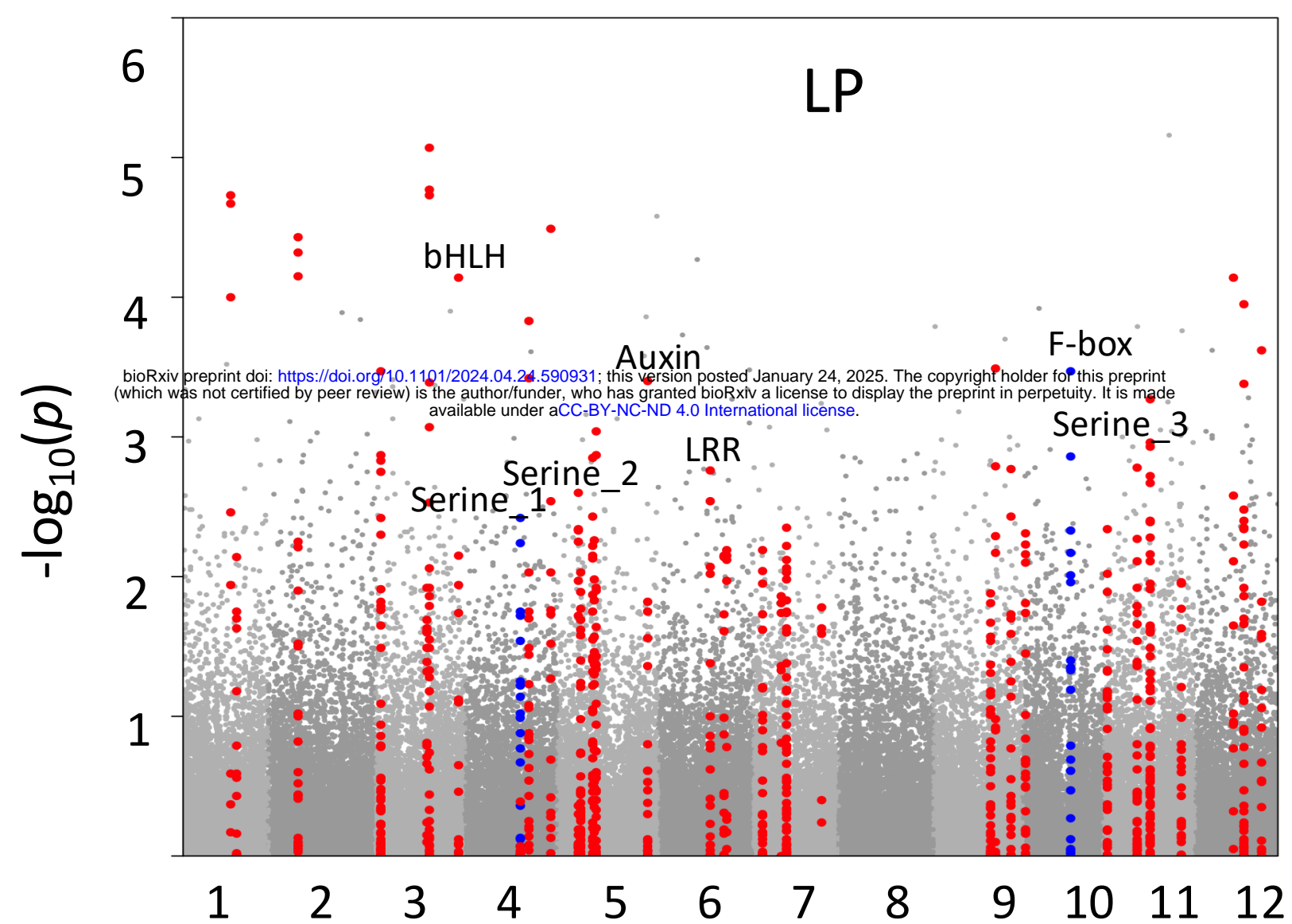
816 Yeatman, C. W. & Teich, A. H. (1969). Genetics and breeding of jack and lodgepole pines in  
817 Canada. *The Forestry Chronicle*, 45(6), 428-433. <https://doi.org/10.5558/tfc45428-6>

818 Zhou, H., Bai, S., Wang, N., Sun, X., Zhang, Y., Zhu, J., & Dong, C. (2020). CRISPR/Cas9-mediated  
819 mutagenesis of MdCNGC2 in apple callus and VIGS-mediated silencing of MdCNGC2 in  
820 fruits Improve resistance to *Botryosphaeria dothidea*. *frontiers in Plant Science*, 11,  
821 575477. <https://doi.org/10.3389/fpls.2020.575477>

822

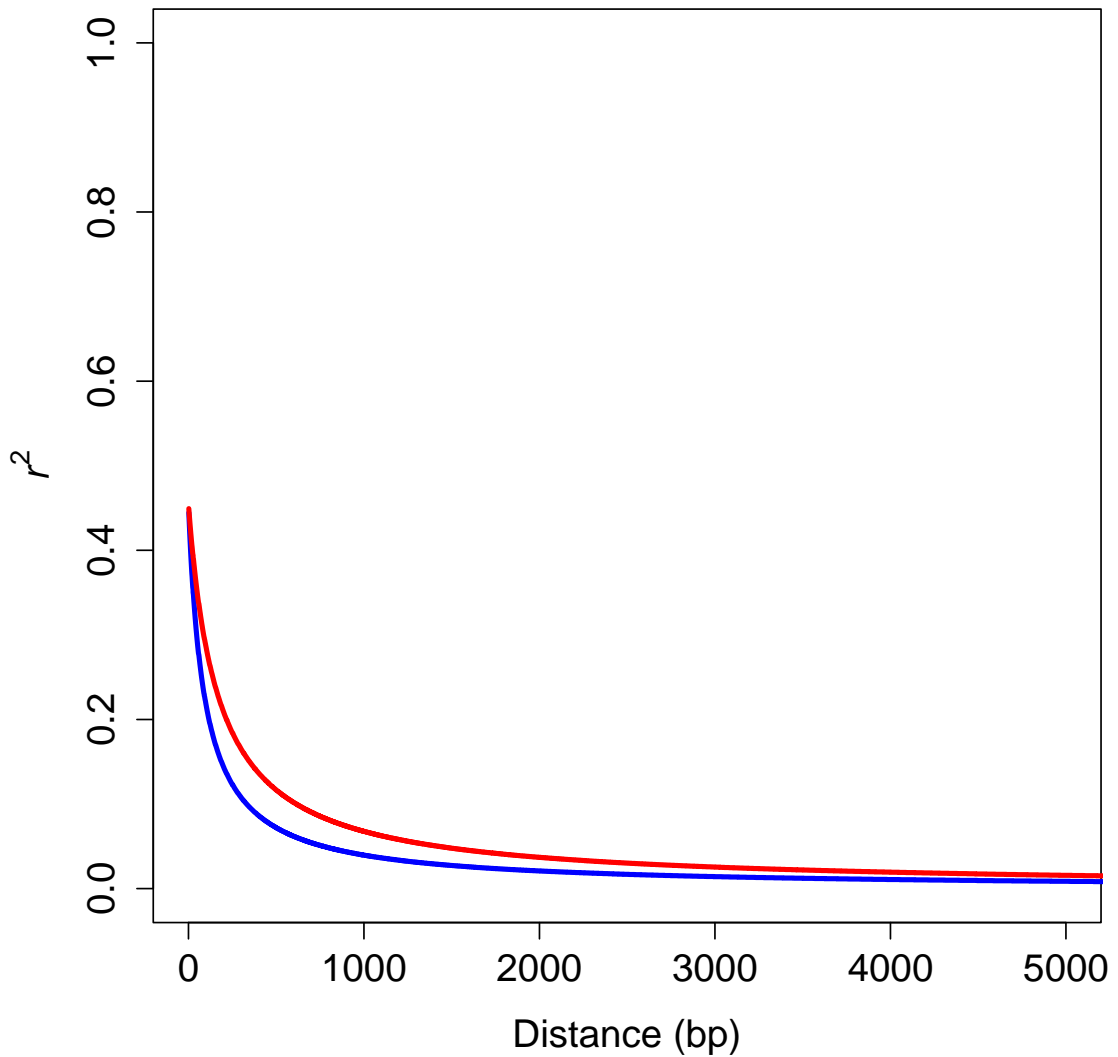






Genome-wide  
Outlier

LP



JP + LPxJP

